Complement C1s cleaves PfEMP1 at interdomain conserved sites inhibiting plasmodium falciparum cytoadherence

Biological Sciences: Microbiology

Complement C1s cleaves PfEMP1 at interdomain conserved sites inhibiting *Plasmodium falciparum* cytoadherence

Yvonne Azasi[1#], Leanne M. Low[1#], Ashley N. Just[2], Sai S. R. Raghavan[2], Christian W. Wang[2], Paola Valenzuela-Leon[1], J. Alexandra Rowe[3], Joseph D. Smith[4,5,6], Thomas Lavstsen[2]*, Louise Turner[2]*, Eric Calvo[1]* and Louis H. Miller[1]*

[1]Laboratory of Malaria and Vector Research, National Institute of Allergy and Infectious Diseases, National Institutes of Health, Rockville, MD 20852, USA. [2]Centre for Medical Parasitology, Department of International Health, Immunology & Microbiology, University of Copenhagen and Department of Infectious Diseases, Rigshospitalet, Copenhagen, Denmark. [3]Institute of Immunology and Infection Research, Centre for Immunity, Infection and Evolution, School of Biological Sciences, Ashworth Laboratories, Kings Buildings, Charlotte Auerbach Rd, Edinburgh, EH9 3FL, UK. [4]Seattle Children's Research Institute, Seattle, WA 98109, USA. [5]Department of Pediatrics, University of Washington, Seattle, WA 98195, USA. [6] Department of Global Health, University of Washington, Seattle, WA 98195, USA

Yvonne Azasi and Leanne M. Low are co-first authors

* Corresponding authors. lmiller@niaid.nih.gov; ecalvo@niaid.nih.gov; lturner@sund.ku.dk; thomasl@sund.ku.dk

Keywords: C1s, PfEMP1, cytoadhesion, EPCR, CD36, ICAM-1, malaria, serum

Abstract

Cytoadhesion of *Plasmodium falciparum* infected erythrocytes (IEs) to the endothelial lining of blood vessels protects parasites from splenic destruction, but also leads to detrimental inflammation and vessel occlusion. Surface display of the *P. falciparum* erythrocyte membrane protein 1 (PfEMP1) adhesion ligands exposes them to host antibodies and serum proteins. PfEMP1 are important targets of acquired immunity to malaria, and through evolution, the protein family has expanded and diversified to bind a select set of host receptors through antigenically diversified receptor-binding domains. Here, we show that complement component 1s (C1s) in serum, cleaves PfEMP1 at semi-conserved arginine motifs located at interdomain regions between the receptor-binding domains, rendering the IE incapable of binding the two main PfEMP1 receptors, CD36 and endothelial protein C receptor (EPCR). Bioinformatic analyses of PfEMP1 protein sequences from 15 *P. falciparum* genomes found the C1s motif was present in most PfEMP1 variants. Prediction of C1s cleavage and loss of binding to endothelial receptors was further corroborated by testing of several different parasite lines. These observations suggest that the parasites have maintained susceptibility for cleavage by the serine protease, C1s, and provides evidence for a complex relationship between the complement system and the *P. falciparum* cytoadhesion virulence determinant.

Significance Statement

Mature asexual stages of *Plasmodium falciparum*-infected erythrocytes (IEs) bind to endothelium to avoid splenic clearance. The PfEMP1 family is the major cytoadhesion ligand at the IE surface and is essential for parasite sequestration. In this study, we show that complement component 1s (C1s), found in serum, cleaves PfEMP1 on the IEs to prevent binding to endothelial cells. We find that the C1s cleavage sites are maintained at semi-conserved arginine motifs located at interdomain regions between PfEMP1 receptor-binding domains and upstream of the transmembrane region. This suggests that parasites have taken advantage of a human serum protease, either to escape antibody recognition of sequestered parasites or to dampen sequestration and pathogenesis from uncontrolled inflammatory responses threatening host survival.

Introduction

Plasmodium falciparum is the most virulent *Plasmodium* spp., causing the most deaths from malarial parasites (1). This virulence is largely due to the parasite´s ability to invade all ages of erythrocytes and its binding to the endothelium. In their late stages, infected erythrocytes (IEs) attach to endothelial cells to escape blood circulation and the killing mechanisms in the spleen (2). The sequestration of IEs in host organs reduces blood flow and promotes coagulopathy, inflammation and vascular leakage (3, 4). In severe infections, sequestration of parasites in the brain may cause breakdown of the blood brain barrier and cerebral edema leading to death or neurologic sequelae to those who survive (2, 5-7).

IE sequestration is mediated by members of the *P. falciparum* erythrocyte membrane protein 1 (PfEMP1) family (8-10), which are exported to the IE surface where they bind specific endothelial receptors. PfEMP1 are single-pass membrane proteins, with the intracellular acidic terminal segment (ATS) anchored in the erythrocyte membrane by intracellular parasite and host cytoskeleton proteins. The PfEMP1 extracellular region can vary in size from 200-500 kDa by the number and type of different receptor binding Duffy binding-like (DBL) and cysteine rich-interdomain region (CIDR) domains (11). Despite varying in sequence, all PfEMP1 contain an N-terminal DBLα-CIDR domain complex, termed the head structure, which segregates the protein family into a few mutually exclusive binding phenotypes (as reviewed in (12)). Thus, most PfEMP1 bind either endothelial protein C receptor (EPCR) via their CIDRα1 domain or CD36 via their CIDRα2-6 domain, and a minority of PfEMP1 head structures have CIDRβ, γ or δ domain types with unknown binding specificity (12). The head structure can be followed by two to seven additional domains. The function of the PfEMP1's C-terminal domains is not fully resolved; however, some bind leukocyte adhesion receptors ICAM-1 (via the DBLβ domain)

(13), platelet endothelial cell adhesion molecule (PECAM1) (14), integrin αVβ3 (15) or hyaluronan-binding protein 1 (HABP1) (16). Other domains have been found to bind serum proteins, non-immune IgG (17) and IgM (18) and α2-macroglobulin (19), facilitating cytoadherence to uninfected erythrocytes (rosetting) and escape from antibody or complement recognition (20). The exception to these rules is the VAR2CSA PfEMP1 variant, which is defined by six tightly connected and unique DBL domains, which form a single multi-domain complex to bind placental chondroitin sulphate A (CSA) (21). Whereas multiple adhesion properties have been mapped to PfEMP1 adhesion domains, less attention has been placed on the interdomain regions, which are characterized by aspartic acid and glutamic acid-rich regions and proline residues, but some also contain conserved motifs (11). The interdomain regions have been thought to function as spacers between the adhesion domains, and a function has not been ascribed to the conserved motifs.

Each parasite genome encodes ~60 PfEMP1 variants, but only one PfEMP1 will be expressed by each individual parasite. PfEMP1 are key targets of acquired immunity to malaria. Expression of one of many variants among parasites released from the liver (22), and the ability to switch PfEMP1 expression at each blood stage cycle, provides the parasite optimal chances of survival regardless of the immune status of the host (8). The PfEMP1 binding phenotypes are linked to clinical outcome of infection. VAR2CSA-mediated sequestration in the placenta is the cause of severe malaria in pregnancy (23, 24), whereas parasites expressing EPCR-binding PfEMP1 is associated with severe malaria pathogenesis in non-immune individuals, and parasites expressing CD36-binding PfEMP1 appear to be linked to uncomplicated infections in semi-immune individuals (25-33).

Pathogens that live in human serum have frequently evolved mechanisms to evade complement-mediated lysis. Expanding literature on complement and malarial parasites is reviewed by Kennedy *et al.* (34). For example, there is evidence that *P. falciparum* merozoites acquire C1 esterase inhibitor during red blood cell invasion to control complement activation (35). The present study was initiated to explain the loss of IE binding to EPCR after exposure to human sera or human plasma from malaria naïve people, but not to bovine sera (30). Previous work suggested the inhibitory serum component(s) was neither albumin nor IgM, and the inhibitory activity persisted after IgG depletion from serum (30). We now show that the serum component, complement 1s (C1s) cleaves PfEMP1 on IEs to prevent adherence of either EPCR or CD36-binding PfEMP1 subsets. We identify C1s cleavage sites at conserved motifs in PfEMP1 located in the unstructured interdomain regions between DBL and CIDR domains but not in VAR2CSA. Using a panel of parasite lines expressing different PfEMP1 variants that did or did not contain the predicted cleavage motif, we were able to demonstrate that binding to endothelial receptors was largely affected in those predicted for cleavage. Unlike the free IEs, IEs bound to EPCR were unaffected by C1s.

Results

C1s cleavage of IT4var19 PfEMP1 inhibits IE binding to EPCR

To identify the serum factor responsible for inhibiting the EPCR-dependent endothelial cell binding of IEs expressing the IT4var19 PfEMP1 variant (30), IgG-depleted serum was separated by size exclusion chromatography into 25 fractions. Two serum fractions, B11 and C3, significantly inhibited binding of *P. falciparum* IT4var19 IEs to a human brain endothelial cell line (Fig. 1A and 1B). Serum proteins in the inhibitory fractions B11 and C3 were identified by MS/MS (Dataset S1) and compared to fractions B9, C1 and C5 eluted before and after the inhibitory fractions. Eight proteins (attractin, C1s, complement component 4b (C4b), complement factor H, IgD, inter-alpha-trypsin inhibitor heavy chain H1 (IT1H1) and H2 (ITIH2) and kappa light chain) were identified as being unique to both inhibitory fractions and absent in non-inhibitory fractions B9, C1, and C5. Of these, only the serine protease C1s (36) significantly inhibited IT4var19 IE binding to endothelial cells (Fig. 1C). Also, C1s inhibited IT4var19 IE-EPCR binding in a concentration dependent manner, with significant binding inhibition at physiological concentration of C1s in serum, 30 μg/mL (37, 38), and no significant inhibitory effect at 3 μg/mL C1s and below (Fig. 2A).

C1s cleavage of arginine-specific bonds in the complement components C2 and C4 is a central process in initiating the proteolytic cascade of the classical complement pathway (39). However, several other human non-complement proteins, including MHC class I, are processed by C1s (40, 41), suggesting a broader function of C1s. The peptide substrate specificity of C1s has been described as [A/S/T][G/V/L][G/A]**R**‖[A/S/V/L] L[G/V/L/R] (39). Of interest, the serine protease thrombin has previously been found to cleave native IT4var19, possibly at a C1s-like motif sequence GLG**R**‖SL located in the interdomain region between the DBLγ and DBLδ

domains based on thrombin cleavage of IT4var19-derived peptides (42). This study also found thrombin could detach IT4var19 IEs already adherent to human lung microvascular endothelial cells. To test C1s reversal of IT4var19 IEs bound to recombinant EPCR, high concentrations of C1s (30, 50 or 100 μg/mL) was added to EPCR-bound IT4var19 IEs but binding to EPCR could not be reversed (Fig. 2B).

To determine if C1s cleaved the IT4var19 PfEMP1 on the IE surface, IEs were incubated with recombinant C1s. Unlike untreated parasites that showed PfEMP1 antibody staining on the IE surface (Fig. 3A), C1s-treated IEs showed no PfEMP1 staining when stained with an antibody to the N-terminal DBLα region of IT4var19 (Fig. 3B). C1s treatment did not affect IE surface detection of VAR2CSA expressing IEs (Fig. 3C and 3D). Together, these observations suggest that C1s cleaves the IT4var19 PfEMP1 variant.

C1s cleaves other PfEMP1 at serine protease motifs in spacer regions separating receptor-binding domains

To further explore and map the C1s cleavage site in PfEMP1 variants, we tested two different PfEMP1 variants where we had clonal parasite lines and matching full-length recombinant ectodomains. The IT4var20 PfEMP1 represents an EPCR binding variant and the IT4var13 represents a dual CD36 and ICAM-1 binding variant. C1s abrogated parasite binding to EPCR and CD36, respectively, whereas ICAM-1 binding by IT4var13 IEs was retained (Fig. 4A and 4B). Quantitative PCR confirmed that *ITvar20* and *ITvar13* transcripts were dominant among expressed IT4 *var* genes in the IT4var20 and IT4var13 parasite lines, respectively (Fig. 4C). This indicated that both types of PfEMP1 variants were susceptible to C1s cleavage, but C1s cleavage of IT4var13 had occurred between the CD36 and ICAM-1 binding domains.

To precisely map the cleavage site, recombinant proteins derived from the full-length ectodomain sequences of the IT4var20 (287 kDa) and IT4var13 (312 kDa) were treated with 50 nM C1s at a 1:1 ratio. C1s cleaved both proteins into two major products (Fig. 5A). Mass spectrometry and N-terminal protein sequencing analysis of these products revealed that C1s cleaved IT4var20 at three closely spaced C1s-like motifs located in the interdomain region between the DBLγ and DBLδ domains (Fig. 5B and Dataset S2). Similarly, the IT4var13 recombinant protein was cleaved at a C1s-like motif located in a shorter 23-amino acid interdomain region between the DBLαCIDRα head structure and the adjacent DBLβ domain (Fig. 5B).

In contrast to full-length recombinant ectodomains, C1s treatment of recombinant PfEMP1 protein spanning the N-terminal head structure (NTS-DBLαCIDRα) of the IT4var20 and the PFD1235w PfEMP1 variants, or single CIDR domains binding EPCR (IT4var19 CIDRα1) or CD36 (IT4var26 CIDRα3) did not result in cleavage (Fig. 6A). Moreover, the recombinant head structure proteins as well as the cleavage products of the full ectodomains retained their receptor binding activity following C1s treatment (Fig. 6B). These results aligned with the observed loss of EPCR binding for IEs expressing IT4var20, and with the loss of CD36 but not ICAM-1 binding for IT4var13-expressing IEs, demonstrating that C1s cleaved at C1s serine protease-like sites located in interdomain regions of diverse PfEMP1 variants.

C1s cleavage motifs are conserved in the interdomain regions of PfEMP1

Previous work has not identified a function for the interdomain regions in PfEMP1 variants (43), although some contain semi-conserved sequence motifs, also termed homology blocks (HBs) (11). Remarkably, three homology blocks that specifically map to the interdomain

regions (HB49, HB134 and HB241) each contain a conserved arginine residue and bear striking resemblance to the canonical C1s cleavage motif (MEROPS - the Peptidase Database (ebi.ac.uk)), and overlapped the observed C1s cleavage sites in IT4var13 and IT4var20 recombinant ectodomains (Fig. 5C). Notably HB49, HB134 and HB241 are all specific to the PfEMP1 interdomain regions.

Since the original definition of PfEMP1 HBs from the reference 3D7 genotype and six partial parasite genomes (11), the full-length PfEMP1 ectodomain sequences have been validated from additional *P. falciparum* genomes using long read sequencing (44). To update the homology blocks, we extracted all interdomain regions from a total of 15 parasite genomes and redefined re-occurring sequence motifs using the MEME tool (45). This approach identified two partially overlapping motifs (MEME1 and 2) overlapping 90% of sequences previously annotated by HB49, HB134 and HB241. Mapping these putative C1s cleavage sites back onto the domain-annotated and aligned PfEMP1 sequences revealed a striking pattern of proposed C1s sites located predominantly mid-PfEMP1 across the protein family and/or upstream of the transmembrane region (Fig. 5D). Overall, 80% of PfEMP1 carried one or more C1s sites with no association to particular PfEMP1 subsets (Fig. 5D), apart from the lack of C1s sites in VAR2CSA and the short unusual VAR3 PfEMP1.

To experimentally validate the bioinformatic predictions of C1s cleavage sites, an additional eight available parasite lines representing EPCR, CD36 or ICAM-1 binding phenotypes were exposed to C1s treatment (Table 1). This showed either no effect or loss of receptor binding in accordance with predicted C1s cleavage sites of the expressed PfEMP1 (Table 1, Fig. S1).

Discussion

To avoid splenic destruction, *P. falciparum*-IEs sequester in the microcirculation. The sequestration phenotype exposes the PfEMP1 adhesion ligands to both antibodies and serum proteins. Unexpectedly, we discovered that most PfEMP1 molecules harbor semi-conserved arginine sequence motifs accessible to serine protease C1s cleavage. The C1s cleavage sites are located in the interdomain region, which are characterized by aspartic acid and glutamic acid-rich regions and thought to function as a spacer between receptor-binding domains. C1s cleavage did not directly affect the DBL and CIDR adhesion domains but did render IEs unable to bind receptors due to loss of functional PfEMP1 domains.

In humans, C1s is present in plasma as a pro-enzyme and has a restricted substrate specificity after activation including its key targets C2 and C4 of the complement cascade (40, 46). In addition, several non-complement substrates for activated C1s have been described, including MHC class I and insulin-like growth factor binding protein 5b (36, 40, 41, 47). However, C1s is able to cleave a broad range of unfolded peptides with semi-constrained sequence motifs (39). Here, we found PfEMP1 was cleaved at sites matching previously defined C1s cleavage sites (39), as well as at closely related motifs. These motifs are common in PfEMP1 variants, located within the interdomain sequence regions, and are particularly enriched upstream of the DBLδ domains in the mid-PfEMP1 regions. Interdomain regions can span up to 200 amino acids and consist mainly of low-complexity runs of proline and acidic aspartic acid and glutamic acid residues (11), broken up by the more distinct C1s-like motifs. This organization predicts a disordered structure, which along with sequence diversity of the C1s-like motifs may prevent antibody recognition. More importantly, its organization may ensure that the residues in the C1s motifs are unfolded and accessible to cleavage. This notion aligns with the

recent Cryo-EM resolution of the full-length VAR2CSA ectodomain (21) showing that its interdomain regions play central roles in folding the quaternary structure of the six-domain large complex required for protein-glycan binding.

Importantly, the abundance and position of the C1s motifs in PfEMP1, strongly suggest that they have been retained in this fast-evolving and highly recombinogenic gene family because they provide the parasite a selective advantage. Thus, *P. falciparum* appears to have adapted cleavage by C1s or indeed other serine proteases, such as thrombin (42), to secure optimal control of its endothelial sequestration process. Further studies will be necessary to determine if other serine proteases in serum, including those of the complement and coagulation cascades, the membrane-anchored serine proteases (48), or even *P. falciparum* derived serine proteases cleave PfEMP1 from the red blood cell membrane.

To sequester in the microcirculation, *P. falciparum*-IEs are exposed to serum proteins. The physiological relevance of the findings reported here is not easily resolved by *in vitro* experiments with their limited resemblance of the human vascular environment. A specific C1s-inhibitor would be important to test, but none exist. However, our study does indicate that the C1s-like sites in PfEMP1 are accessible to serine protease cleavage *in vitro*. Whether such proteolytic cleavage of PfEMP1 occurs *in vivo* is a key question raised by our data. The complement cascade is under tight regulation to avoid consumption of complement proteins and activated C1s would usually be inhibited by C1 esterase inhibitor. During malaria infection, complement is activated (49, 50) and complement regulatory proteins are depleted (49, 51, 52). Therefore, PfEMP1 proteins at the IE surface may be exposed to activated serine proteases, such as complement C1s and thrombin, which then cleave PfEMP1 and interfere with cytoadhesion *in vivo*. As complement and coagulation pathways are likely to be more active during high burden

parasite infections, we hypothesize that the extent of PfEMP1 cleavage will be influenced by local concentrations of serine proteases.

We propose two hypothetical mechanisms explaining the conserved C1s cleavage of PfEMP1. First, it is possible that PfEMP1 cleavage serves as an immune escape mechanism in which antibody-opsonized PfEMP1 molecules are released to avoid killing of early trophozoite-stage IEs passing through the spleen or to avoid opsonization of adherent IE by inflammatory cells, such as NK cells (53) or infiltrating monocytes in peripheral blood vessels. The latter scenario aligns with the finding that C1s did not release bound IE and that some C-terminal PfEMP1 DBLε and DBLζ domains, which typically would remain on the IE following C1s cleavage, bind serum proteins α2-macroglobulin and non-immune IgG, IgM to shield the IE from complement or antibody mediated opsonization (17-20). Secondly, and as previously suggested, cleavage by C1s or other serine proteases such as thrombin may act as a "steam valve" mechanism to dampen IE sequestration efficiency in hosts with uncontrolled systemic inflammation (3) threatening survival of the host and parasite. In support of this theory, Gillrie *et al.* found thrombin to release adherent IEs (42); however, in the one case studied, C1s did not release adherent IEs.

Various studies have shown decreased serum activity and levels of complement components in malaria, including C1q which together with a C1s2-C1r2 tetramer forms the Ca^{2+}-dependent C1 complex (37, 54-57). It is possible that reduction in C1s during malaria infection modulates PfEMP1 function. Future studies to assess plasma levels of activated C1s in malaria patients should be possible, and suggestions that proteases could be used therapeutically to reverse sequestration (42) could be explored.

We have described a new and unexpected aspect of the endless battle for survival between the malaria parasite and its host. A better understanding of the role of C1s in the pathogenesis of malaria is needed to determine if it may protect from most severe disease by cleaving PfEMP1 and reducing cytoadhesion or whether C1s and other serum proteases have been hijacked by the parasite to escape immune attack.

Materials and Methods

Parasite and brain endothelial cell culture

IT4 parasites that predominantly express IT4var19 PfEMP1 (27, 30) were kept in continuous culture with O^+ human red blood cells (Interstate Blood Bank, Memphis, TN) at 2% hematocrit in Roswell Park Memorial Institute medium (RPMI) 1640 (CUS-0645; KD Medical, Columbia, MD) supplemented with 0.25% albumax (11021; Thermo Fisher Scientific, San Jose, CA), 5% pooled human serum (Interstate Blood Bank, Memphis, TN), 50 µg/mL gentamicin (KD Medical, Columbia, MD) and 2.0 g/L sodium bicarbonate (KD Medical, Columbia, MD). FCR3-CSA parasites (predominantly expressing VAR2CSA PfEMP1), 3G8 (IT4var1) (58), ItG ICAM-1 (IT4var16) (58), P6G2 (IT4var31) (58), P2E11 (IT4var33) (58), P6D12 (IT4var39/67) (58), and 3173-S parasites predominantly expressing an EPCR-binding PfEMP1 (59) were cultured in RPMI 1640 supplemented with 0.5% albumax, 50 µg/mL gentamicin and 2.0 g/L sodium bicarbonate. Parasite lines derived from the IT4 parasite genotype predominantly expressing IT4var20 or IT4var13 or from the genome reference 3D7 parasite genotype (predominantly expressing MAL6P1.316) were cultured in RPMI 1640 supplemented with 0.5% albumax, 4 mM L-glutamine (G7513; Sigma-Aldrich, St. Louis, MO), and 50 µg/mL gentamicin (G1272; Sigma-Aldrich, St. Louis, MO) with PfEMP1-expression maintained by alternate antibody selection using rat anti-rIT4VAR20/rIT4var13 antibodies and panning on HBMEC

(IT4var20) or CHO-ICAM-1 cells (IT4var13), respectively as previously described (29). For the IT4var20 and IT4var13 parasite lines, analysis of *var* gene expression was done by quantitative PCR as previously described (60). All parasite lines were cultured in 5% O_2, 5% CO_2 and 90% N gas mixture with the exception of 3173-S parasites (cultured in 1% O_2, 5% CO_2 and 94% N gas mixture) and IT4var13 and IT4var20, which were cultured in 2% O_2, 5.5% CO_2 and 92.5% N gas mixture.

Human brain endothelial cells, HBEC-5i (ATCC® CRL-3245™; ATCC, Manassas, VA) cells were cultured as previously described (61). Briefly, the cells were cultured on 0.1% gelatin coated tissue flask in Dulbecco's Modified Eagle's Medium (DMEM)/ Nutrient Mixture F-12 medium (D6421; Sigma-Aldrich, St. Louis, MO) supplemented with 2 mM L-glutamine (A2916801; ThermoFisher Scientific, San Jose, CA), 100 U/mL penicillin/0.1 mg/mL streptomycin (15140122; ThermoFisher Scientific, San Jose, CA), 10% v/v heat-inactivated fetal bovine serum, HI-FBS (16140071; ThermoFisher Scientific, San Jose, CA) and 1% v/v endothelial cell growth supplement (1052; ScienCell, Carlsbad, CA), pH 7.4 at 37°C in 5% CO_2.

IE adhesion assays to endothelial cells

IE binding to a human brain endothelial cell line, HBEC-5i, was done as previously described (30). Briefly, 2% hematocrit of gelatin purified mature trophozoite-stage IEs in DMEM binding medium [bicarbonate-free DMEM/Nutrient Mixture F-12 Ham (D8900; Sigma-Aldrich, St. Louis, MO), supplemented with 2 mM L-glutamine and 100 U/mL penicillin/0.1 mg/mL streptomycin, pH 7.3] were co-incubated with confluent HBEC-5i in 48-well plates at 37 °C for 75 mins with gentle rocking of the plate every 30 mins. Unbound IEs were washed off and

the bound cells were fixed with 2% glutaraldehyde and stained with 5% Giemsa. The cells were counted at 40x with a Zeiss Axio Vert A1 inverted microscope (Zeiss, Oberkochen, Germany).

For binding inhibition assays, serum and serum fractions (at 10%), recombinant human attractin (7238-AT-050; Novus Biologicals, Centennial, CO), C1s (A104; Complement Technology, Tyler, TX or 2060-SE; R&D Systems, Minneapolis, MN), human complement C4b (H00000721-Q01; Novus Biologicals, Centennial, CO), human complement factor H (H00003075-P03; Novus Biologicals, Centennial, CO), IgD (NB100-62667; Novus Biologicals, Centennial, CO), human kappa light chain (H00003514-P01; Novus Biologicals, Centennial, CO), human inter-alpha-trypsin inhibitor heavy chain H1 (IT1H1) (H00003697-P01; Novus Biologicals, Centennial, CO) and H2 (ITIH2) (NBP2-31750PEP; Novus Biologicals, Centennial, CO) (at physiological concentrations in serum, ~10% of the physiological concentrations or an estimated concentration where serum levels could not be found, Table S1) were added to the parasites in DMEM binding medium immediately before co-incubation with HBEC-5i.

IE adhesion assays to receptor molecules immobilized on plastic

The receptor-binding assays were conducted as previously described (30). Plastic plates were spotted with 5 µL of EPCR (13320-H02H; Sino Biologicals, Wayne, PA), CSA (a gift from Dr. Michal Fried), CD36 (1955-CD; R&D Systems, Minneapolis, MN) or ICAM-1 (720-IC; R&D Systems, Minneapolis, MN); all recombinant proteins, except for ICAM-1 which was used at 100 µg/mL, were at a concentration of 50 µg/mL. PBS acted as the negative control. Plates were incubated at 4°C overnight in a humidified box, after which they were blocked with 3% BSA in PBS for 2 h at 37°C. After blocking, a liquid blocker super PAP pen (71312; Electron Microscopy Sciences, Hatfield, PA) was used to draw circles around each spot to ensure that

parasite suspensions with differing concentrations of C1s were contained and did not leak onto other spots. Gelatin-enriched IEs were suspended at 2% hematocrit in binding medium (bicarbonate-free DMEM-F12 Ham (D8900; Sigma)/0.1% BSA, pH 7.2-7.4). Parasites were incubated with or without the desired concentration of C1s (0.03 µg/mL – 30 µg/mL) for 30 mins at 37°C. Subsequently, the parasites were added to the appropriate spots and incubated for 1 h at 37°C, with resuspension every 12 mins by gently swirling the dish. Unbound IEs were washed off with binding medium, whilst adherent cells were fixed with 2% glutaraldehyde for 1 h and stained with 5% Giemsa for 10 min. Bound IEs were counted by light microscopy with a 40x objective, with three fields being counted per spot.

Static binding assay for IT4var20 IEs and IT4var13 IEs were as previously described (62). Briefly, late trophozoite and schizont stages were purified using Magnetic Cell Sorting (MACS, Miltenyi Biotec, Germany), and adjusted to 4 x 10^6 cells/mL in 2% FCS (in PBS). Parasites were pre-incubated 1 h with or without 100 µg/mL of rC1s (204879; Sigma-Aldrich, St. Louis, MO) before being added to petri dishes (BD Falcon 351029) coated with spots of 20 µL of 20 µg/mL rEPCR (63), CD36 (SRP6378; Sigma-Aldrich, St. Louis, MO), ICAM-1 (64) or 2% BSA (A7030; Sigma-Aldrich, St. Louis, MO). After one hour of incubation at 37°C, unbound parasites were washed away, while bound parasites were fixed with glutaraldehyde, stained with Giemsa and counted.

For assays investigating the reversal of IE bound to EPCR or CSA, the receptor-binding portion was conducted as stated above; however, spots were incubated with the parasite suspension for 45 mins at 37°C. After washing of unbound IEs with binding medium, C1s (30 µg/mL – 100 µg/mL) in binding medium was added to the appropriate spot and incubated at

37°C for another 45 mins. The spots were then gently washed with binding medium and bound IEs were fixed, stained, and counted as described above.

C1s treatment of IEs and immunofluorescent assay

Gelatin-purified IT4var19 and FCR3 pigmented trophozoite-stage IEs were washed twice with RPMI and treated with 100 nM (8 μg/mL) C1s at 2% hematocrit in RPMI at 37°C for 2 hrs. IEs in RPMI only with no C1s were included as controls. The IT4var19 and FCR3 IEs were washed three times with PBS and stained with 25 μg/mL anti-IT4var19 NTS.DBLα rabbit IgG (27) and anti-FCR3VAR2CSA (full length) rat IgG diluted in 1% BSA/PBS, respectively. A "no antibody" control was included with both parasite lines. The parasites were incubated at 4°C for 1 hr, washed three times in PBS and stained with a 1:500 dilution of Alexa Fluor 488 goat anti-rabbit IgG (A-11008; Life Technologies, Carlsbad, CA) or Alexa Fluor 594 goat anti-rat IgG (A-11007 Invitrogen, Carlsbad, CA) in PBS/1% BSA at 4°C for 45 mins. The parasites were washed three times in PBS, smeared onto glass slides and air dried. The slides were mounted in ProLong Gold Antifade Mountant with DAPI (P36935; Invitrogen, Carlsbad, CA), covered with cover slips and sealed with Cytoseal-60 (8310-4; ThermoFisher Scientific, San Jose, CA). The cells were viewed using a Zeiss laser scanning microscope (LSM) 880 microscope (Zeiss, Oberkochen, Germany) with AiryScan at 63×/1.4NA. The optical resolution of the captured images was enhanced isometrically by ~1.8-fold through automatic processing with the Zen software.

Fractionation of serum samples by high-performance liquid chromatography (HPLC)

IgG was depleted from heat-inactivated serum as previously described by binding IgG in serum to a protein G column and collecting the IgG depleted flow through (30) . The IgG-depleted serum samples were fractionated by HPLC using a Superdex 200 10/300 GL column (GE Healthcare, Piscataway, NJ) and the AKTA Purifier system. Proteins were eluted isocratically at a flow rate of 0.5 mL/min in 1X PBS. Absorbance was monitored at 220 and 280 nm and fractions were collected in a 96-well plate with 1 min of interval.

Liquid chromatography/mass spectroscopy (LC/MS) of serum

Active fractions (B11 and C3) and inactive, lateral fractions (B9, C1 and C5) from Superdex 200 chromatography were submitted for protein identification by LC/MS at the Research Technology Branch Core Facility of the NIAID. Mass spectrometry was performed on reduced and alkylated, trypsin digested samples prepared by standard mass spectrometry protocols. The supernatant and two washes (5% formic acid in 50% acetonitrile) of the gel digests were pooled and concentrated with a Speed Vac (Labconco, Kansas, MO) to dryness directly in 200 µl polypropylene auto-sampler vials (Sun Sri, Rockwood, TN). The peptides were re-suspended in 10 µl of Solvent A (98% water; 2% acetonitrile; 0.1% formic acid) prior to mass spectrometry acquisitions. Samples were acquired on an Orbitrap Fusion Tribrid mass spectrometer (ThermoFisher Scientific, San Jose, CA) equipped with an EASY-Spray Ion Source and an Easy-nLC 1000. The nano-LC was carried out on an ES0802 analytical column (2µm/75 µm /25 cm) at 60C and a PepMap C18 Trap column operating a linear gradient over 80 mins from 100% mobile phase A to 40% mobile phase B (98% acetonitrile;2% water;0.1% formic acid), a ramp to 80% B over 2 mins and a final hold at this concentration for additional 2 mins.

Acquisitions were performed in data dependent mode with a cycle time of 3 secs with a full MS scan of all ions from m/z 400 to mz/ 1800 at a resolution of 120,000 (m/z 190 at the target value of 4E5). The most intense precursor ions were fragmented in the Ion Trap using an isolation window of 1 m/z, a q of 0.25, and CID collision energy of 35%. Dynamic exclusion was enabled with the duration of 15 sec with ± 10 ppm mass tolerance. Raw files were searched using PEAKS v8.5 (BSi, Waterloo, Canada) against a Uniprot KB database containing Human, Pig and Cow proteins (02/2018) and common contaminants (cRAP.fasta, theGPM.org). Peptides were filtered at a 0.5% peptide FDR with a 2 peptide per protein minimum. Quantitation was performed using a Top 3 approach.

Recombinant protein analyses

Recombinant PfEMP1 proteins were produced in baculovirus-infected insect cells as previously described (29, 63, 65). Newly designed N-terminal "head-structure" proteins spanned from start 1-Methionine to a 728-Cysteine (~85 kDa) of the PFD1235w variant and from 1-Methionine to 724-Cysteine 724 (~84 kDa) of the IT4var20 variant.

Proteins were treated with 50 nM (4 µg/mL) C1s in 1:1 molar ratio for 1 hr and analyzed by SDS PAGE. Analysis of recombinant PfEMP1 protein binding to human receptors, endothelial protein C receptor (63), ICAM-1 (64) and CD36 was performed using ELISA as previously described (29, 65, 66). In short, ELISA plates were coated either with human receptor (3 µg/mL) or recombinant PfEMP1 (5, 15 or 30 µg/mL for single domains, head structure or full length ectodomian PfEMP1 proteins, respectively). After blocking, coated proteins were incubated with recombinant PfEMP1 or human receptor at said concentrations for 1 hr. Human receptors were detected using HRP-conjugated streptavidin and recombinant PfEMP1 proteins

were detected using HRP-conjugated anti-V5 tag antibodies. All analyses were performed in duplicates.

Liquid chromatography–mass spectrometry and N-terminal protein sequencing of C1s cleaved PfEMP1 protein

C1s cleavage products of IT4var13 and IT4var20 were excised from SDS page gels, subjected to in-gel tryptic digestion and analyzed by reverse phase liquid chromatography and Shotgun Mass-Spectrometry. In-gel digested peptides were loaded onto a 15 cm x 75 µm PepMap™RSLC column packed with 2 µm C18 beads (ES803A; Thermo Fisher Scientific, San Jose, CA), using EASY-nLC 1200 chromatography system with a 2 cm x 75 µm, Acclaim®PepMap100 trap column, packed with 3 µm, C18 beads. The peptides were eluted from the column in a mixture of Solvent A (0.1% Formic Acid (LS118-212; Fisher Scientific, Hampton, NH) and Solvent B (80% Acetonitrile, 0.1% Formic Acid (15431423; Fisher Scientific, Hampton, NH) at 250 nL/min rate. The chromatographic gradient was from 6% to 60% Solvent B in 45 mins (from 6% to 23% in 20 mins; from 23% to 38% in 10 mins; from 38% to 60% in 3 mins; followed by wash steps from 60% to 95% in 5 mins and 95% Solvent B for 7 mins). Shotgun MS was performed using a Q Exactive Mass spectrometer (Thermo Fisher Scientific, San Jose, CA) operated in data-dependent acquisition mode for 70min. MS1 resolution of 70.000, AGC target set to 3e6, maximum injection time set to 20 ms, scan range 300 to 1750 m/z, selecting the Top 10 MS1 ions for MS2 analysis. MS2 scans used 17,500 resolution, AGC target of 1e6, maximum injection time 60ms, and isolation window of 1.6 m/z at normalized collision energy of 25. Minimum AGC target was set to 1e3 and dynamic exclusion at 30 s. MS data analysis was performed using Proteome Discoverer 2.4, searching the

IT4var20 and IT4var13 sequences. The database was concatenated with one composed of all protein sequences in reversed order. We applied 10 ppm precursor ion tolerance for total protein level identification and 0.02 Da for fragment ion tolerance using SEQUEST search algorithm and Percolator for FDR filtering. Carbamidomethylation of cysteine residues (+57.021 Da) was set as a static modification, while Oxidation (+15.995 Da) was set as a variable modification. Peptide-spectrum matches (PSM's) did not exceed 1% false discovery rate (FDR). Filtered PSM's were further filtered for peptide and protein-level FDR of 1%. Data output is given in Dataset S2.

For Edman N-terminal sequencing, C1s-treated IT4var20 ectodomain was dissolved in LDS buffer with DTT and heated at 70°C for 10 mins. The sample was loaded onto the NuPAGE 12% Bis-Tris gel and separated with MOPS running buffer at 200V for 50 mins. The gel was blotted onto a PVDF membrane and stained with Ponceau. The ~95 kDa band of interest was cut out and analyzed by N-terminal Edman sequencing of five residues using an ABI Procise 494 sequencer. Raw data can be found in Dataset S2.

Bioinformatic analyses

PfEMP1 interdomain sequences were extracted from domain-annotated PfEMP1 protein sequences of 15 *P. falciparum* genomes assembled from PacBio long-read-sequencing data ftp.sanger.ac.uk/pub/project/pathogens/Plasmodium/falciparum/PF3K/ (44). Reoccurring protein sequence motifs in the interdomain sequences were identified using MEME, meme-suite.org/meme/tools/meme (45), by searching for the 32 most abundant motifs of minimum four residues in length. The Position-Specific Scoring Matrix (PSSM) for each of two identified C1s-like motifs (MEME1 and MEME2) are given in Dataset S2 and formatted ready for use in MEME (https://meme-suite.org/meme/). As such they can be used to identify putative C1s-

cleavage sites in any PfEMP1 sequence e.g., using the MEME "Find Individual Motif Occurrences" FIMO function. These were used for mapping C1s-like sites back on onto full-length PfEMP1 sequences. Figure 5 shows C1s site positions in 275 representative domain annotated PfEMP1 sequences.

Statistical analysis

All data were statistically analyzed and graphed using GraphPad Prism 8. Data are presented as mean ± SEM. Data were log transformed and an unpaired two-tailed T-test was performed to compare groups to the positive binding control. For comparison of the eight potential candidates to control (Fig. 1C), an ordinary one-way ANOVA was performed with Dunnett's test.

Acknowledgements

We thank Drs. Michal Fried, Patrick Duffy and Yai Doritchamou (NIAID, NIH) for the FCR3 parasites, FCR3VAR2CSA rat antibody and CSA. We are also grateful to Drs. Lisa Renee Olano and Glenn Nardone of the Protein Chemistry Section, Research Technologies Branch, NIAD, NIH for their assistance in proteomics analysis and to Dr. Anja TR Jensen (Department of Immunology and Microbiology, University of Copenhagen) for recombinant ICAM-1. We thank Dr. Michael P. Fay (NIAID, NIH) for his advice on statistical analysis. The study was supported by the Intramural Research Program of NIAID/NIH, Kirsten og Freddy Johansens Fond, Læge Sofus Carl Emil Friis og hustru Olga Doris Friis Fond, The Lundbeck Foundation, The Independent Research Fund Denmark, and by funds from NIH grant R01AI141602 (JDS).

References

1. W. H. Organization (2020) World malaria report 2020: 20 years of global progress and challenges. (World Health Organization, Geneva).
2. A. R. Jensen, Y. Adams, L. Hviid, Cerebral Plasmodium falciparum malaria: The role of PfEMP1 in its pathogenesis and immunity, and PfEMP1-based vaccines to prevent it. *Immunol Rev* **293**, 230-252 (2020).
3. S. Portugal *et al.*, Exposure-dependent control of malaria-induced inflammation in children. *PLoS Pathog* **10**, e1004079 (2014).
4. C. A. Moxon *et al.*, Loss of endothelial protein C receptors links coagulation and inflammation to parasite sequestration in cerebral malaria in African children. *Blood* **122**, 842-851 (2013).
5. R. Idro, N. E. Jenkins, C. R. Newton, Pathogenesis, clinical features, and neurological outcome of cerebral malaria. *Lancet Neurol* **4**, 827-840 (2005).
6. B. A. Riggle *et al.*, CD8+ T cells target cerebrovasculature in children with cerebral malaria. *J Clin Invest* **130**, 1128-1138 (2020).
7. T. E. Taylor *et al.*, Differentiating the pathologies of cerebral malaria by postmortem parasite counts. *Nat Med* **10**, 143-145 (2004).
8. J. D. Smith *et al.*, Switches in expression of Plasmodium falciparum var genes correlate with changes in antigenic and cytoadherent phenotypes of infected erythrocytes. *Cell* **82**, 101-110 (1995).
9. D. I. Baruch *et al.*, Cloning the P. falciparum gene encoding PfEMP1, a malarial variant antigen and adherence receptor on the surface of parasitized human erythrocytes. *Cell* **82**, 77-87 (1995).

10. X. Z. Su *et al.*, The large diverse gene family var encodes proteins involved in cytoadherence and antigenic variation of Plasmodium falciparum-infected erythrocytes. *Cell* **82**, 89-100 (1995).

11. T. S. Rask, D. A. Hansen, T. G. Theander, A. Gorm Pedersen, T. Lavstsen, Plasmodium falciparum erythrocyte membrane protein 1 diversity in seven genomes--divide and conquer. *PLoS Comput Biol* **6** (2010).

12. J. D. Smith, J. A. Rowe, M. K. Higgins, T. Lavstsen, Malaria's deadly grip: cytoadhesion of Plasmodium falciparum-infected erythrocytes. *Cell Microbiol* **15**, 1976-1983 (2013).

13. J. D. Smith *et al.*, Identification of a Plasmodium falciparum intercellular adhesion molecule-1 binding domain: a parasite adhesion trait implicated in cerebral malaria. *Proc Natl Acad Sci U S A* **97**, 1766-1771 (2000).

14. Q. Chen *et al.*, The semiconserved head structure of Plasmodium falciparum erythrocyte membrane protein 1 mediates binding to multiple independent host receptors. *J Exp Med* **192**, 1-10 (2000).

15. O. Chesnokov, J. Merritt, S. O. Tcherniuk, N. Milman, A. V. Oleinikov, Plasmodium falciparum infected erythrocytes can bind to host receptors integrins alphaVbeta3 and alphaVbeta6 through DBLdelta1_D4 domain of PFL2665c PfEMP1 protein. *Sci Rep* **8**, 17871 (2018).

16. A. Magallon-Tejada *et al.*, Cytoadhesion to gC1qR through Plasmodium falciparum Erythrocyte Membrane Protein 1 in Severe Malaria. *PLoS Pathog* **12**, e1006011 (2016).

17. K. Flick *et al.*, Role of nonimmune IgG bound to PfEMP1 in placental malaria. *Science* **293**, 2098-2100 (2001).

18. J. P. Semblat *et al.*, Identification of the minimal binding region of a Plasmodium falciparum IgM binding PfEMP1 domain. *Mol Biochem Parasitol* **201**, 76-82 (2015).

19. L. Stevenson *et al.*, alpha2-Macroglobulin Can Crosslink Multiple Plasmodium falciparum Erythrocyte Membrane Protein 1 (PfEMP1) Molecules and May Facilitate Adhesion of Parasitized Erythrocytes. *PLoS Pathog* **11**, e1005022 (2015).

20. R. R. Akhouri, S. Goel, H. Furusho, U. Skoglund, M. Wahlgren, Architecture of Human IgM in Complex with P. falciparum Erythrocyte Membrane Protein 1. *Cell Rep* **14**, 723-736 (2016).

21. R. Ma *et al.*, Structural basis for placental malaria mediated by Plasmodium falciparum VAR2CSA. *Nat Microbiol* 10.1038/s41564-020-00858-9 (2021).

22. A. Bachmann *et al.*, Controlled human malaria infection with Plasmodium falciparum demonstrates impact of naturally acquired immunity on virulence gene expression. *PLoS Pathog* **15**, e1007906 (2019).

23. M. Fried, P. E. Duffy, Adherence of Plasmodium falciparum to chondroitin sulfate A in the human placenta. *Science* **272**, 1502-1504 (1996).

24. A. Salanti *et al.*, Selective upregulation of a single distinctly structured var gene in chondroitin sulphate A-adhering Plasmodium falciparum involved in pregnancy-associated malaria. *Mol Microbiol* **49**, 179-191 (2003).

25. T. Lavstsen *et al.*, Plasmodium falciparum erythrocyte membrane protein 1 domain cassettes 8 and 13 are associated with severe malaria in children. *Proc Natl Acad Sci U S A* **109**, E1791-1800 (2012).

26. M. Bernabeu *et al.*, Severe adult malaria is associated with specific PfEMP1 adhesion types and high parasite biomass. *Proc Natl Acad Sci U S A* **113**, E3270-3279 (2016).

27. A. Claessens *et al.*, A subset of group A-like var genes encodes the malaria parasite ligands for binding to human brain endothelial cells. *Proc Natl Acad Sci U S A* **109**, E1772-1781 (2012).

28. M. Avril *et al.*, A restricted subset of var genes mediates adherence of Plasmodium falciparum-infected erythrocytes to brain endothelial cells. *Proc Natl Acad Sci U S A* **109**, E1782-1790 (2012).

29. L. Turner *et al.*, Severe malaria is associated with parasite binding to endothelial protein C receptor. *Nature* **498**, 502-505 (2013).

30. Y. Azasi *et al.*, Infected erythrocytes expressing DC13 PfEMP1 differ from recombinant proteins in EPCR-binding function. *Proc Natl Acad Sci U S A* **115**, 1063-1068 (2018).

31. J. Storm *et al.*, Cerebral malaria is associated with differential cytoadherence to brain endothelial cells. *EMBO Mol Med* **11** (2019).

32. J. S. Jespersen *et al.*, Plasmodium falciparum var genes expressed in children with severe malaria encode CIDRalpha1 domains. *EMBO Mol Med* **8**, 839-850 (2016).

33. A. Kessler *et al.*, Linking EPCR-Binding PfEMP1 to Brain Swelling in Pediatric Cerebral Malaria. *Cell Host Microbe* **22**, 601-614 e605 (2017).

34. A. T. Kennedy, C. Q. Schmidt, W.-H. Tham, "Complement Evasion Mechanisms of the Human Pathogen Plasmodium falciparum" in Complement Activation in Malaria Immunity and Pathogenesis, J. A. Stoute, Ed. (Springer International Publishing, Cham, 2018), 10.1007/978-3-319-77258-5_6, pp. 107-124.

35. A. T. Kennedy *et al.*, Recruitment of Human C1 Esterase Inhibitor Controls Complement Activation on Blood Stage Plasmodium falciparum Merozoites. *J Immunol* **198**, 4728-4737 (2017).

36. P. Gal, G. Ambrus, P. Zavodszky, C1s, the protease messenger of C1. Structure, function and physiological significance. *Immunobiology* **205**, 383-394 (2002).

37. N. R. Cooper, B. J. Fogel, Complement in acute experimental malaria. II. Alterations in the components of complement. *Mil Med* **131**, Suppl:1180-1190 (1966).

38. M. T. Amano *et al.*, Genetic analysis of complement C1s deficiency associated with systemic lupus erythematosus highlights alternative splicing of normal C1s gene. *Mol Immunol* **45**, 1693-1702 (2008).

39. F. K. Kerr *et al.*, Elucidation of the substrate specificity of the C1s protease of the classical complement pathway. *J Biol Chem* **280**, 39510-39514 (2005).

40. Z. Fishelson, "Complement Factor B" in xPharm: The Comprehensive Pharmacology Reference, S. J. Enna, D. B. Bylund, Eds. (Elsevier, New York, 2007), https://doi.org/10.1016/B978-008055232-3.63066-1, pp. 1-8.

41. H. Eriksson, Proteolytic cleavage of MHC class I by complement C1-esterases--an overlooked mechanism? *Immunotechnology* **2**, 163-168 (1996).

42. M. R. Gillrie *et al.*, Thrombin Cleavage of Plasmodium falciparum Erythrocyte Membrane Protein 1 Inhibits Cytoadherence. *mBio* **7** (2016).

43. J. D. Smith, G. Subramanian, B. Gamain, D. I. Baruch, L. H. Miller, Classification of adhesive domains in the Plasmodium falciparum erythrocyte membrane protein 1 family. *Mol Biochem Parasitol* **110**, 293-310 (2000).

44. T. D. Otto *et al.*, Long read assemblies of geographically dispersed Plasmodium falciparum isolates reveal highly structured subtelomeres. *Wellcome Open Res* **3**, 52 (2018).

45. T. L. Bailey, J. Johnson, C. E. Grant, W. S. Noble, The MEME Suite. *Nucleic Acids Res* **43**, W39-49 (2015).

46. N. M. Thielens, C. Gaboriaud, V. Rossi, "Chapter 11 - C1s" in The Complement FactsBook (Second Edition), S. Barnum, T. Schein, Eds. (Academic Press, 2018), https://doi.org/10.1016/B978-0-12-810420-0.00011-0, pp. 107-115.

47. W. H. Busby, Jr. *et al.*, The complement component C1s is the protease that accounts for cleavage of insulin-like growth factor-binding protein-5 in fibroblast medium. *J Biol Chem* **275**, 37638-37644 (2000).

48. T. M. Antalis, G. D. Conway, R. J. Peroutka, M. S. Buzza, Membrane-anchored proteases in endothelial cell biology. *Curr Opin Hematol* **23**, 243-252 (2016).

49. T. Srichaikul, P. Puwasatien, J. Karnjanajetanee, V. A. Bokisch, P. Pawasatien, Complement changes and disseminated intravascular coagulation in Plasmodium falciparum malaria. *Lancet* **1**, 770-772 (1975).

50. M. Roestenberg *et al.*, Complement activation in experimental human malaria infection. *Trans R Soc Trop Med Hyg* **101**, 643-649 (2007).

51. J. N. Waitumbi, B. Donvito, A. Kisserli, J. H. Cohen, J. A. Stoute, Age-related changes in red blood cell complement regulatory proteins and susceptibility to severe malaria. *J Infect Dis* **190**, 1183-1191 (2004).

52. J. N. Waitumbi, M. O. Opollo, R. O. Muga, A. O. Misore, J. A. Stoute, Red cell surface changes and erythrophagocytosis in children with severe plasmodium falciparum anemia. *Blood* **95**, 1481-1486 (2000).

53. G. Arora *et al.*, NK cells inhibit Plasmodium falciparum growth in red blood cells via antibody-dependent cellular cytotoxicity. *Elife* **7** (2018).

54. B. J. Fogel, A. E. Von Doenhoff, Jr., N. R. Cooper, E. H. Fife, Jr., Complement in acute experimental malaria. I. Total hemolytic activity. *Mil Med* **131**, Suppl:1173-1179 (1966).

55. F. A. Neva *et al.*, Relationship of serum complement levels to events of the malarial paroxysm. *J Clin Invest* **54**, 451-460 (1974).

56. B. M. Greenwood, M. J. Brueton, Complement activation in children with acute malaria. *Clin Exp Immunol* **18**, 267-272 (1974).

57. P. Phanuphak *et al.*, Complement changes in falciparum malaria infection. *Clin Exp Immunol* **59**, 571-576 (1985).

58. J. H. Janes *et al.*, Investigating the host binding signature on the Plasmodium falciparum PfEMP1 protein family. *PLoS Pathog* **7**, e1002032 (2011).

59. M. Bernabeu *et al.*, Binding Heterogeneity of Plasmodium falciparum to Engineered 3D Brain Microvessels Is Mediated by EPCR and ICAM-1. *mBio* **10** (2019).

60. C. W. Wang *et al.*, Evidence for in vitro and in vivo expression of the conserved VAR3 (type 3) plasmodium falciparum erythrocyte membrane protein 1. *Malar J* **11**, 129 (2012).

61. A. Claessens, J. A. Rowe, Selection of Plasmodium falciparum parasites for cytoadhesion to human brain endothelial cells. *J Vis Exp* 10.3791/3122, e3122 (2012).

62. P. A. Magistrado *et al.*, High efficacy of anti DBL4varepsilon-VAR2CSA antibodies in inhibition of CSA-binding Plasmodium falciparum-infected erythrocytes from pregnant women. *Vaccine* **29**, 437-443 (2011).

63. C. K. Lau *et al.*, Structural conservation despite huge sequence diversity allows EPCR binding by the PfEMP1 family implicated in severe childhood malaria. *Cell Host Microbe* **17**, 118-129 (2015).

64. A. Bengtsson *et al.*, Transfected HEK293 cells expressing functional recombinant intercellular adhesion molecule 1 (ICAM-1)--a receptor associated with severe Plasmodium falciparum malaria. *PLoS One* **8**, e69999 (2013).

65. F. L. Hsieh *et al.*, The structural basis for CD36 binding by the malaria parasite. *Nat Commun* **7**, 12837 (2016).

66. G. K. Cham *et al.*, A semi-automated multiplex high-throughput assay for measuring IgG antibodies against Plasmodium falciparum erythrocyte membrane protein 1 (PfEMP1) domains in small volumes of plasma. *Malar J* **7**, 108 (2008).

Figure legends

Figure 1. Serum fractions B11 and C3 inhibit IT4var19 IE binding to brain endothelial cells. (A) Chromatographic fractionation of serum by size-exclusion chromatography. IgG-depleted serum was run on a Superdex 200 Increase 10/300 GL column. Protein fractions were eluted using a linear gradient and the absorbance (mAbs) monitored at 280 nm. The arrows show the binding inhibitory fractions B11 and C3. (B) Binding of IT4var19 IEs to HBEC-5i in binding medium with 10% human serum, IgG-depleted human serum, or serum fractions (A6-C6). A no serum control was included. Each data point is from two independent experiments done in duplicate and the mean and SEM are shown for each fraction. Fractions B11 and C3 most affected the binding. These fractions were run on MS/MS and the components were run to determine their effect on binding as shown in (C) to identify potential inhibitors for binding. **(**C) Binding of IT4var19 IEs to HBEC-5i in binding medium with proteins identified by MS/MS in the serum inhibitory B11 and C3 fractions (attractin, C1s, C4b, factor H, IgD, IT1H1, ITIH2 and kappa light chain). Data are mean ± SEM, and each data point is from an independent experiment. ** P<0.01; *** P<0.001.

Figure 2. C1s inhibits binding of IT4var19 IEs to EPCR but does not reverse binding of bound IEs. (A) Binding of IT4var19 IEs to EPCR in the absence or presence of C1s (0.03 μg/mL – 30 μg/mL). (B) No evidence of the reversal of IT4var19 IEs bound to EPCR in the presence of C1s (30 μg/mL – 100 μg/mL). The mean and SEM are shown, and each data point is from an independent experiment. All mean values were log-transformed, and a two-tailed unpaired t-test was conducted to compare C1s treated groups to the positive control (EPCR only). ** P<0.01; *** P<0.001.

Figure 3. C1s cleaves the native PfEMP1 on the surface of IT4var19 IEs. Staining of (A) IT4var19 IEs, (B) C1s treated IT4var19 IEs, (C) FCR3 (VAR2CSA) and (D) C1s-treated FCR3 (VAR2CSA) with rabbit polyclonal IgG to IT4var19 NTS.DBLα or rat polyclonal IgG to FCR3 full length VAR2CSA. IEs were identified by DAPI staining of parasite nuclei (blue). IT4var19 PfEMP1 staining of the IEs is shown in green and FCR3 VAR2CSA PfEMP1 staining is shown in red.

Figure 4. C1s inhibits binding of IT4var20 IE to EPCR and IT4var13 IE binding to CD36 but not ICAM-1. (A) Binding of IT4var20 IEs to EPCR in the absence or presence of C1s (100 μg/mL). Recombinant EPCR (rEPCR) was included as a control and indicator of how well C1s treatment abrogated IT4var20 binding to EPCR. (B) Binding of IT4var13 IEs to CD36 or ICAM-1 in the absence or presence of C1s (100 μg/mL). In both binding assays, bovine serum albumin (BSA) was included as a negative control. The mean and SEM are shown, and each data point is from an independent experiment. For statistical testing, all mean values were log-transformed, and a two-tailed unpaired t-test was conducted to compare experimental groups to the positive control (EPCR only). (C) *Var* gene transcript levels relative to the housekeeping control gene, seryl-t-transferase, confirming the major *var* types being expressed as IT4var20 and IT4var13. * $P<0.05$; ** $P<0.01$; ns – not significant.

Figure 5. Analysis of observed and predicted C1s cleavage sites in PfEMP1.
(A) SDS page showing C1s cleaves the full-length recombinant ectodomains of IT4var13 and IT4var20 PfEMP1 into two major bands (arrows, numbered 1 to 4). (B) Protein schematics of the

IT4var13 and IT4var20 ectodomains showing the C1s cleavage products (black arrows, above the protein schematic from panel (A). The boxed insets show the interdomain sequences where C1s cleavage sites were identified in IT4var13 and IT4var20 by LS/MS and N-terminal protein sequencing analyses. C1s cleaves at one site in IT4var13 and three sites in IT4var20 (red arrows) at residues (large amino acid letters) resembling C1s-motifs. Of the four C1s-like sequence motifs found in IT4var20, three (red arrows) in (B) were experimentally confirmed and the fourth site (green arrow) in panel (B) may also have been cleaved but could not be validated due to its presence in a small peptide product lost in gel-electrophoresis. (C) C1s cleavage sites in PfEMP1 resemble previously identified semi-conserved sequence motifs, known as homology blocks HB49, HB134 and HB241(11), found in the otherwise low sequence complexity interdomain regions of PfEMP1. (D) Reanalysis of conserved sequence motifs in PfEMP1 interdomains from 15 long-read sequenced *P. falciparum* genomes using MEME confirms the presence of C1s-like cleavage motifs (sequence LOGOs shown at left). The right side shows 275 representative full-length PfEMP1 from 15 PacBio long-read sequenced *P. falciparum* genomes (44). The different PfEMP1 are stacked from top to bottom in three columns and aligned by their domain composition (not scaled to sequence length). Each domain type is color-coded and white gaps between domains represent interdomain regions, which may vary from 10 to 225 amino acids in length. Interdomain regions containing one or more predicted C1s-like cleavage sites (MEMEs 1 and 2) are indicated by red crosses. NTS = N-terminal segment at the beginning of protein, ATS = acidic terminal segment or cytoplasmic tail.

Figure 6. Analysis of C1s-treated recombinant PfEMP1. (A) SDS page gel showing two representative PfEMP1 CIDR domains (EPCR-binding IT4var19 CIDRα1 and CD36-binding

CIDRα3) and two EPCR-binding head-structure domain complexes (PFD1235w [NTSA-DBLα1-CIDRα1] and IT4var20 [NTSA-DBLα1-CIDRα1]) before and after treatment with 50 nM C1s at 1:1 molar ratio for 1 hr at 37˚C. No proteolysis was seen. (B) ELISA data showing the effect of 50 nM C1s pre-treatment on binding of recombinant PfEMP1 proteins to coated EPCR, CD36 or ICAM-1 (filled boxes) versus EPCR binding to coated recombinant PfEMP1 (hashed boxes). Whereas C1s treatment reduced binding activity of full length PfEMP1 ectodomains, recombinant PfEMP1 head structure domains are insensitive to C1s treatment, indicating that C1s cleavage sites are located in the interdomain regions, consistent with mass spectrometry analysis. As a control, C1s treatment of EPCR did not affect its binding to full-length PfEMP1 ectodomains (hashed boxes).

Table legends.

Table 1: Summary of predicted and observed C1s effects on studied parasites lines.

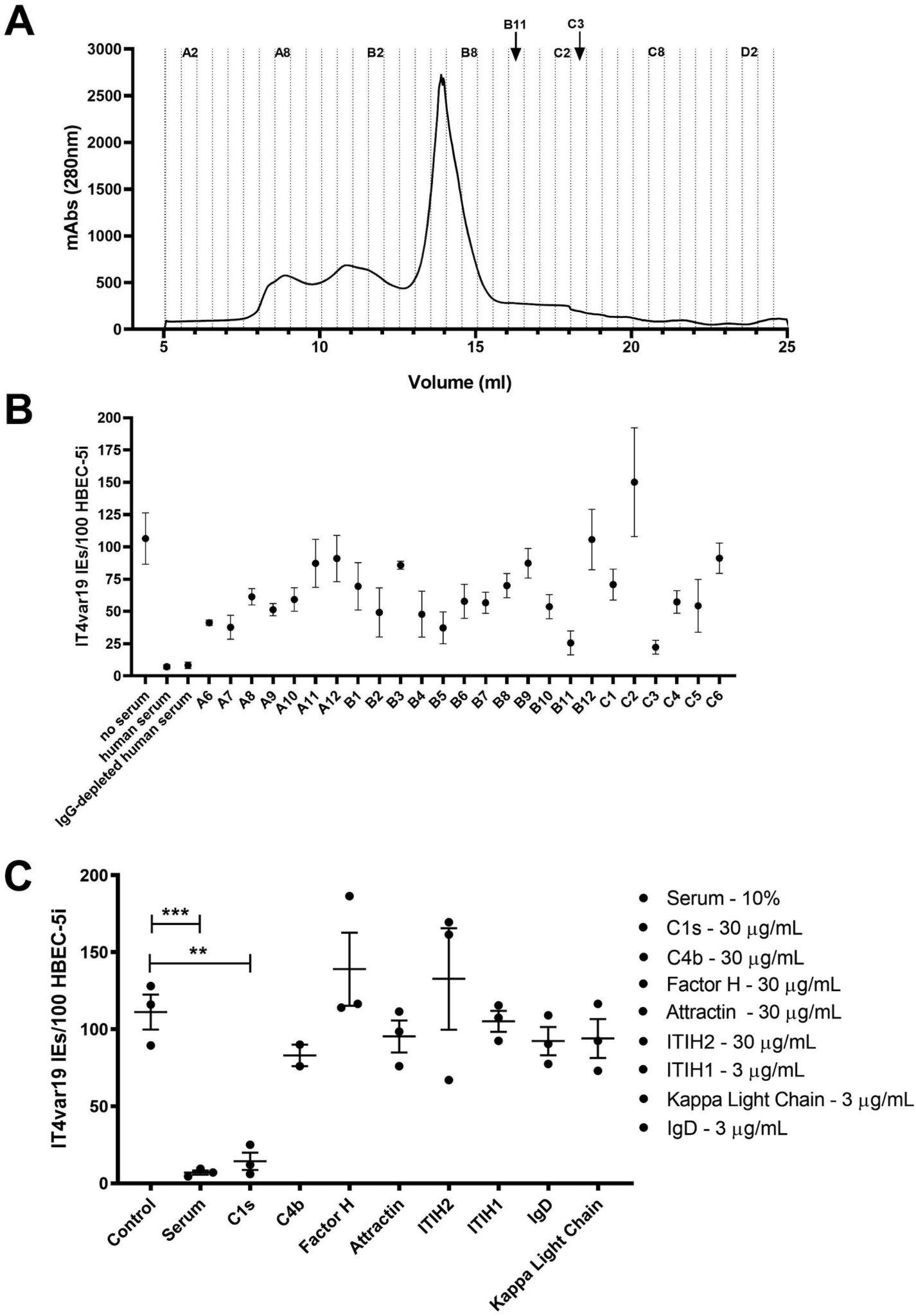
A
B11
C3
A2
A8
B2
B8
C2
C8
D2
3000
2500
2000
1500
1000
500
0
mAbs (280nm)
5
10
15
20
25
Volume (ml)
B
IT4var19 IEs/100 HBEC-5i
200
175
150
125
100
75
50
25
0
no serum
human serum
IgG-depleted human serum
A6
A7
A8
A9
A10
A11
A12
B1
B2
B3
B4
B5
B6
B7
B8
B9
B10
B11
B12
C1
C2
C3
C4
C5
C6
C
IT4var19 IEs/100 HBEC-5i
200
150
100
50
0
***
**
Control
Serum
C1s
C4b
Factor H
Attractin
ITIH2
ITIH1
IgD
Kappa Light Chain
Serum - 10%
C1s - 30 μg/mL
C4b - 30 μg/mL
Factor H - 30 μg/mL
Attractin - 30 μg/mL
ITIH2 - 30 μg/mL
ITIH1 - 3 μg/mL
Kappa Light Chain - 3 μg/mL
IgD - 3 μg/mL

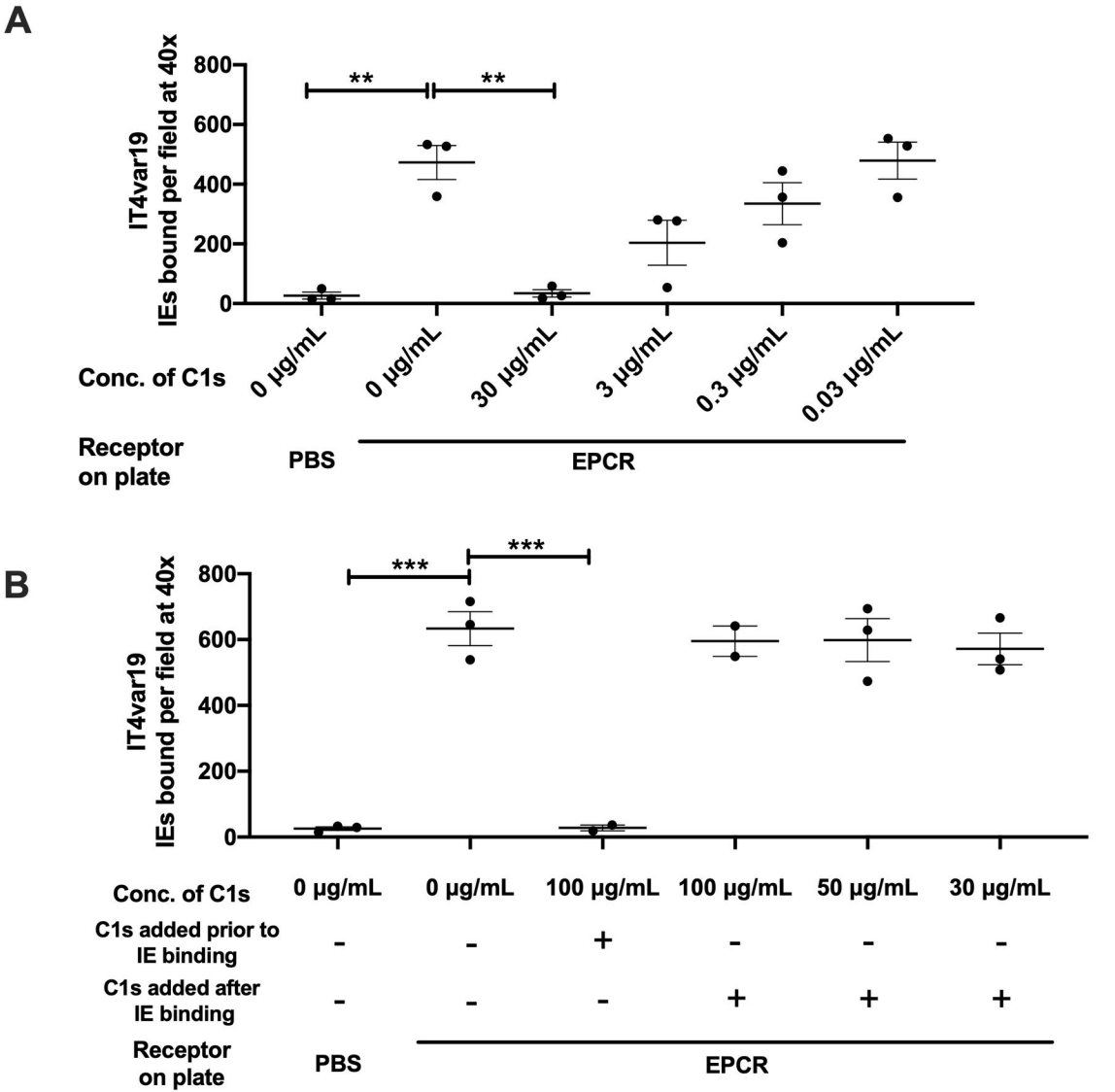
A
IT4var19
IEs bound per field at 40x
800
600
400
200
0
**
**
Conc. of C1s
0 µg/mL
0 µg/mL
30 µg/mL
3 µg/mL
0.3 µg/mL
0.03 µg/mL
Receptor
on plate
PBS
EPCR
B
IT4var19
IEs bound per field at 40x
800
600
400
200
0
***
***
Conc. of C1s
0 µg/mL
0 µg/mL
100 µg/mL
100 µg/mL
50 µg/mL
30 µg/mL
C1s added prior to IE binding
- - + - - -
C1s added after IE binding
- - - + + +
Receptor
on plate
PBS
EPCR

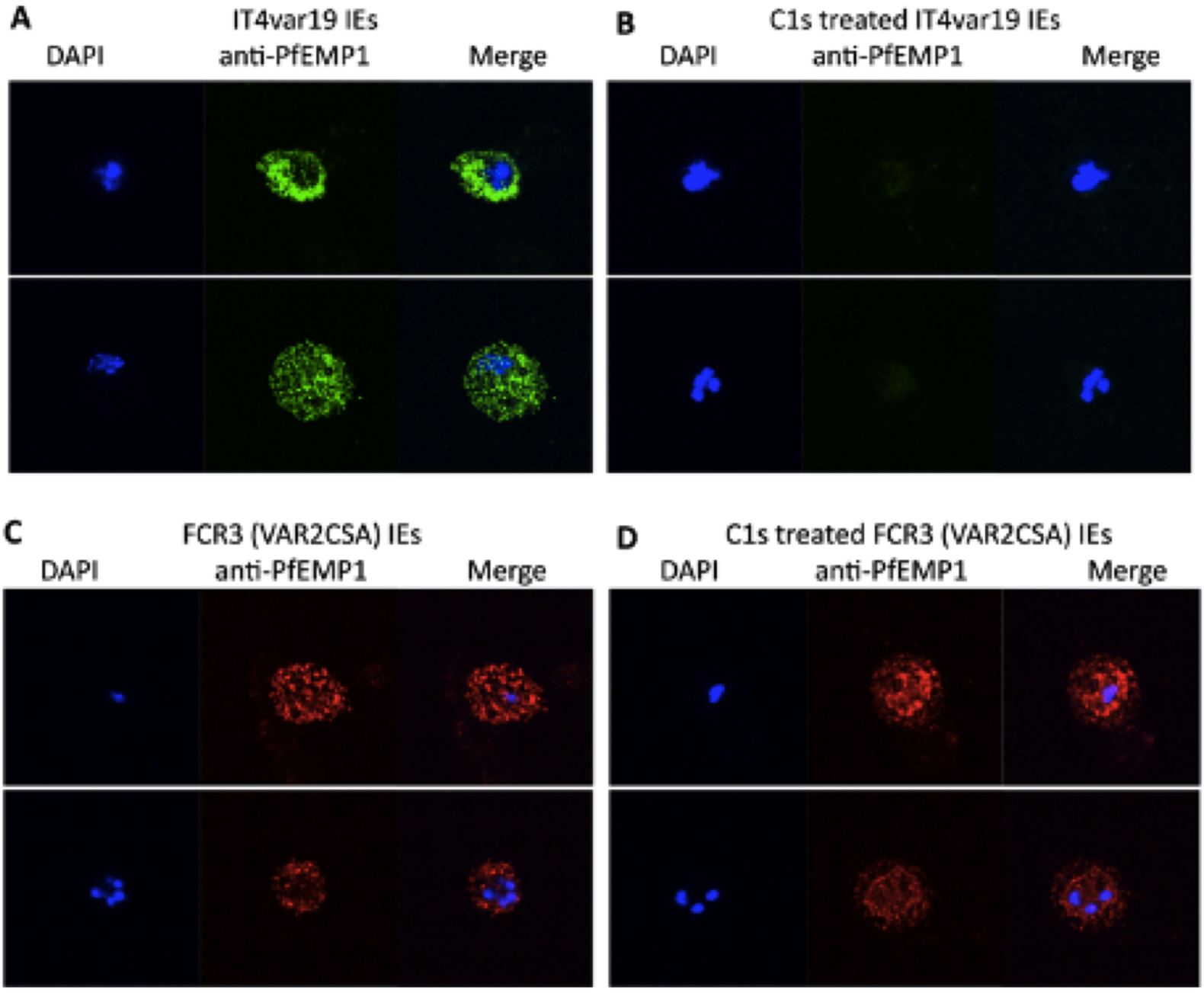
A
IT4var19 IEs
DAPI
anti-PfEMP1
Merge
B
C1s treated IT4var19 IEs
DAPI
anti-PfEMP1
Merge
C
FCR3 (VAR2CSA) IEs
DAPI
anti-PfEMP1
Merge
D
C1s treated FCR3 (VAR2CSA) IEs
DAPI
anti-PfEMP1
Merge

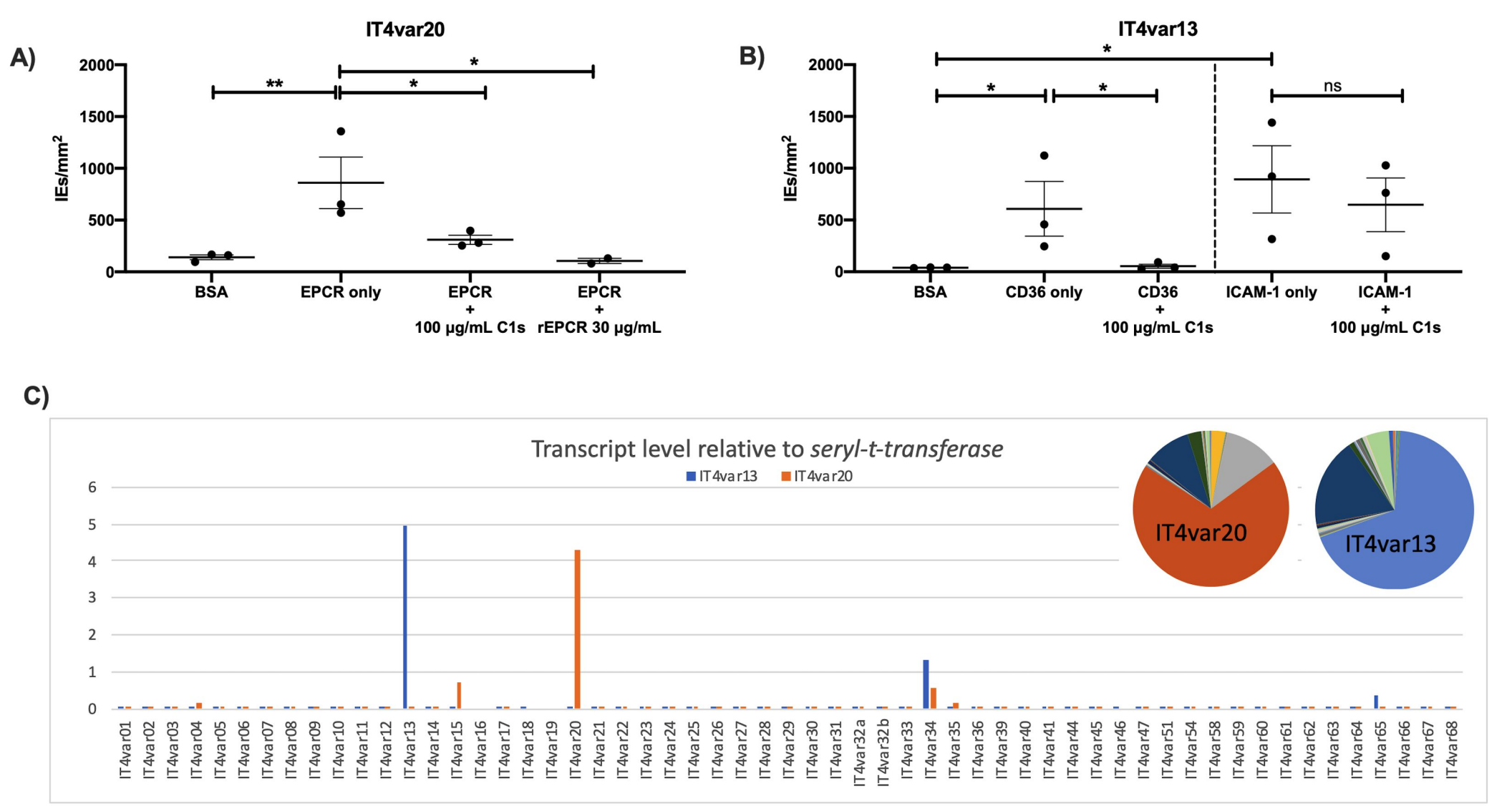
A)
IT4var20
IEs/mm2
2000
1500
1000
500
0
**
*
*
BSA
EPCR only
EPCR + 100 µg/mL C1s
EPCR + rEPCR 30 µg/mL
B)
IT4var13
IEs/mm2
2000
1500
1000
500
0
*
*
*
ns
BSA
CD36 only
CD36 + 100 µg/mL C1s
ICAM-1 only
ICAM-1 + 100 µg/mL C1s
C)
Transcript level relative to seryl-t-transferase
IT4var13
IT4var20
6
5
4
3
2
1
0
IT4var20
IT4var13
IT4var01 IT4var02 IT4var03 IT4var04 IT4var05 IT4var06 IT4var07 IT4var08 IT4var09 IT4var10 IT4var11 IT4var12 IT4var13 IT4var14 IT4var15 IT4var16 IT4var17 IT4var18 IT4var19 IT4var20 IT4var21 IT4var22 IT4var23 IT4var24 IT4var25 IT4var26 IT4var27 IT4var28 IT4var29 IT4var30 IT4var31 IT4var32a IT4var32b IT4var33 IT4var34 IT4var35 IT4var36 IT4var39 IT4var40 IT4var41 IT4var44 IT4var45 IT4var46 IT4var47 IT4var51 IT4var54 IT4var58 IT4var59 IT4var60 IT4var61 IT4var62 IT4var63 IT4var64 IT4var65 IT4var66 IT4var67 IT4var68

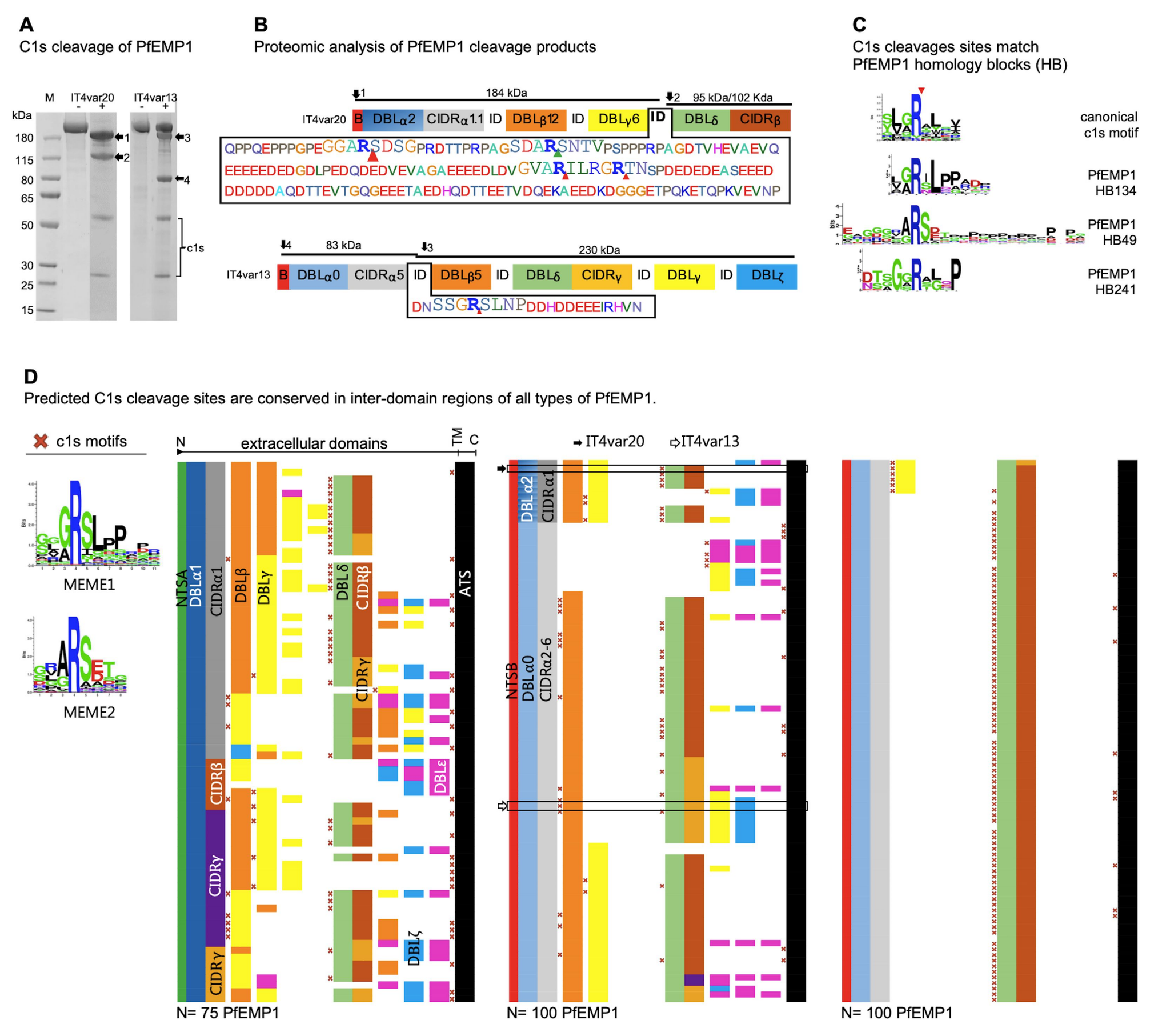
A
C1s cleavage of PfEMP1
M
IT4var20
IT4var13
kDa
180
115
80
65
50
30
25
15
c1s
B
Proteomic analysis of PfEMP1 cleavage products
184 kDa
95 kDa/102 Kda
IT4var20
DBLα2
CIDRα1.1
DBLβ12
DBLγ6
DBLδ
CIDRβ
QPPQEPPPGPEGGARSDSGPRDTTPRPAGSDARSNTVPSPPPRPAGDTVHEVAEVQ
EEEEEDEDGDLPEDQDEDVEVAGAEEEEDLDVGVARILRGRTNSPDEDEDEASEEED
DDDDDAQDTTEVTGQGEEETAEDHQDTTEETVDQEKAEEDKDGGGETPQKETQPKVEVNP
83 kDa
230 kDa
IT4var13
DBLα0
CIDRα5
DBLβ5
DBLδ
CIDRγ
DBLγ
DBLζ
DNSSGRSLNPDDHDDEEEIRHVN
C
C1s cleavages sites match
PfEMP1 homology blocks (HB)
canonical
c1s motif
PfEMP1
HB134
PfEMP1
HB49
PfEMP1
HB241
D
Predicted C1s cleavage sites are conserved in inter-domain regions of all types of PfEMP1.
c1s motifs
MEME1
MEME2
N
extracellular domains
TM
C
IT4var20
IT4var13
NTSA
DBLα1
CIDRα1
DBLβ
DBLγ
DBLδ
CIDRβ
CIDRγ
DBLε
DBLζ
ATS
NTSB
DBLα0
CIDRα2-6
N= 75 PfEMP1
N= 100 PfEMP1
N= 100 PfEMP1

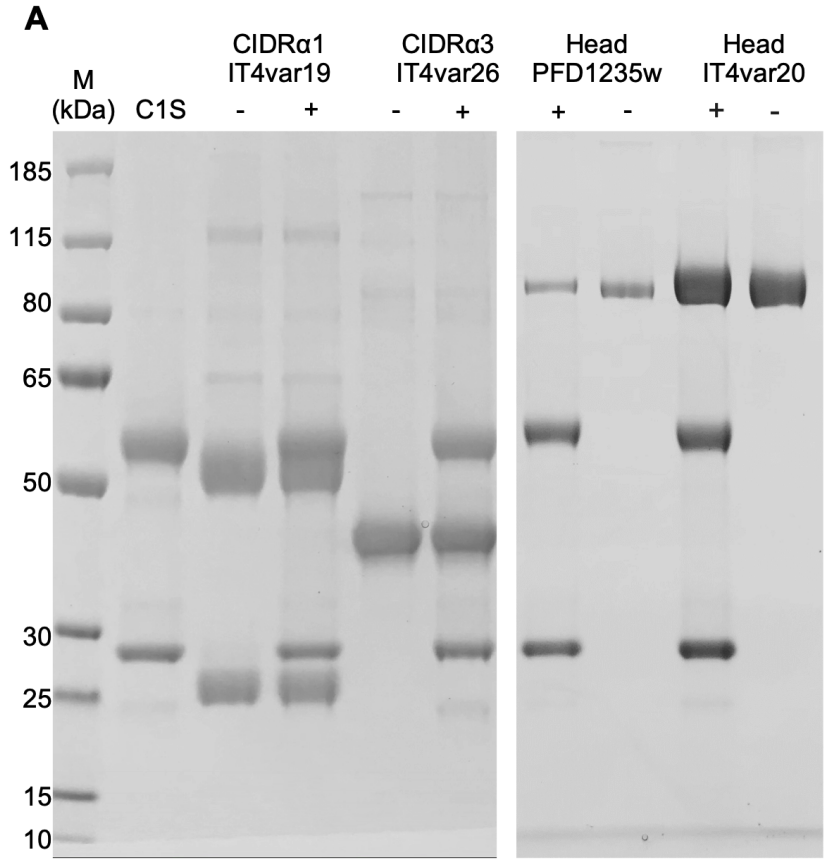
A
M
(kDa)
C1S
CIDRα1
IT4var19
CIDRα3
IT4var26
Head
PFD1235w
Head
IT4var20
- + - + + - + -
185
115
80
65
50
30
25
15
10

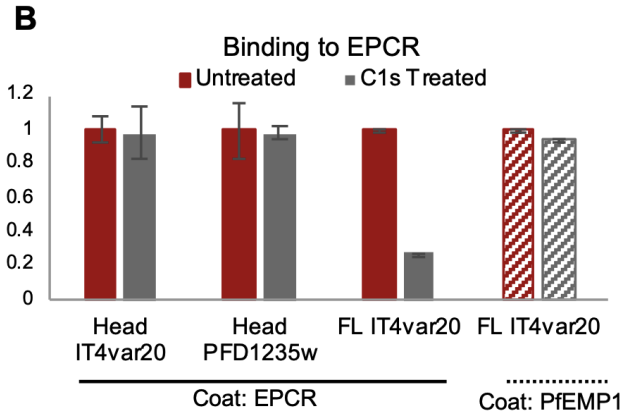
B
Binding to EPCR
Untreated
C1s Treated
1.2
1
0.8
0.6
0.4
0.2
0
Head IT4var20
Head PFD1235w
FL IT4var20
FL IT4var20
Coat: EPCR
Coat: PfEMP1

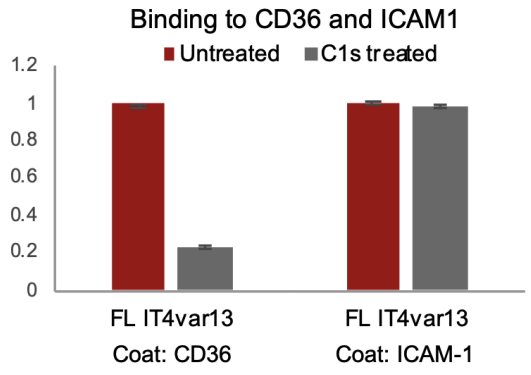
Binding to CD36 and ICAM1
Untreated
C1s treated
1.2
1
0.8
0.6
0.4
0.2
0
FL IT4var13
Coat: CD36
FL IT4var13
Coat: ICAM-1

Table 1: Summary of predicted and observed C1s effects on studied parasite lines.

Parasite name/*var* gene	Predicted C1s cleavage site?	Binding ligand	Predicted inhibition of binding by C1s?	Observed inhibition by C1s (≥30µg/mL)?	p value	Full length recombinant protein cleaved?
IT4var19	Yes	EPCR	Yes	Yes	***	ND
IT4var20	Yes	EPCR	Yes	Yes	*	Yes
3D7 MAL6P1.316	Yes	EPCR	Yes	Yes	*	ND
3173-S	ND[a]	EPCR	ND	Yes[#]	*	ND
IT4var13	Yes[b]	CD36	Yes	Yes	**	Yes
		ICAM-1	No	No	ns	
3G8 (IT4var1)	No	CD36	No	No	ns	ND
		ICAM-1	No	No	ns	
ItG ICAM-1 (IT4var16)	No	CD36	No	No	ns	ND
		ICAM-1	No	No	ns	
P6G2 (IT4var31)	No	CD36	No	No	ns	ND
P2E11 (IT4var33)	Yes	CD36	Yes	Yes	**	ND
P6D12 (IT4var39/67)	Yes	CD36	Yes	Yes	**	ND
FCR3 (VAR2CSA)	No	CSA	No	No	ns	ND

* $p<0.05$, ** $p<0.01$; *** $p<0.001$
ns – not significant
ND – Not determined
[a] – Full sequence not available yet for prediction. Partial Sequence available – GenBank: QBH72553.1
[b] – predicted cleavage between CD36 and ICAM-1 binding domains
[#] - binding assay conducted with HBEC-5i.